Chapter 3

Extracellular Glutathione and RBC Metabolism

3.1 Background

Glutathione is the most abundant low molecular weight thiol-containing molecule in mammalian cells (Cotgreave and Gerdes, 1998). It is maintained in its reduced form by glutathione reductase (GR), an NADPH-dependent enzyme. Under normal conditions ~99% of the total glutathione in healthy RBCs exists as GSH (Tietze, 1969). The oxidised forms are GSSG and mixed disulfides of glutathione with proteins and other thiols (GSSR). These species can interconvert non-enzymatically or are reduced to GSH by GR and glutaredoxin (Meister and Anderson, 1983). Glutathione participates in multiple reactions in the cell: it acts as an intracellular thiol buffer (Filomeni, *et al.*, 2002), it protects the cell against ROS and other intracellular oxidants (Meister and Anderson, 1983), acts as a co-substrate for detoxifying enzymes such as GSHPx, GST and glyoxalase I (Rae, *et al.*, 1990; Cotgreave and Gerdes, 1998), and increases the rate of PMOR activity in the face of oxidative stress (May, *et al.*, 2001b). Hence as well as GSH being implicated in protection against UV-induced ROS (Moral, *et al.*, 2000), its redox status has frequently been used as a measure of oxidative stress (Filomeni, *et al.*, 2002).

Plasma concentrations of glutathione are generally in the low micromolar range, with 90% of it existing as the reduced form (Jeevanandam, *et al.*, 2000). Steady-state plasma concentrations derive from a balance between liver secretion, and uptake and degradation by other tissues (Jeevanandam, *et al.*, 2000). Although the liver is the main endogenous secretor of GSH, both GSH and GSSG are also released by other cell types in response to oxidative stress (Thom, *et al.*, 1997), glucose deprivation (Regan and Guo, 1999) and nitrite addition (Lapshina and Bartosz, 1995). RBCs

release GSH in response to oxidative stress induced by peroxynitrite but not that induced by superoxide or nitric oxide (Thom, *et al.*, 1997). This peroxynitrile induced release of GSH is inhibited by glucose, maltose and cytochalisin B, suggesting that released GSH protects essential exofacial thiol groups on the hexose transporter (Thom, *et al.*, 1997). Oxidants that have been shown to induce GSSG export from RBC, include hydrogen peroxide, tBHP, PMS and sodium nitrite (Lapshina and Bartosz, 1995). GSH is also released from neurons undergoing ischaemia via a Ca^{2+}-mediated process (Regan and Guo, 1999). Micromolar concentrations of extracellular GSH activate the *N*-methyl-D-aspartate receptor and decrease neuronal survival rates when these cells are exposed to oxidative stress (Regan and Guo, 1999).

The manner in which cells respond to extracellular GSH or GSSG *in vitro* appears to depend on the type of cell and its redox status. Cancer cell growth is inhibited by extracellular GSH in a cell-line specific manner: the ovarian carcinoma cell line A2780, but not the IGROV-1 cell line, is sensitive to extracellular GSH-induced DNA damage and apoptosis (Perego, *et al.*, 2000). In contrast, extracellular GSH appears to play a protective role in the case of rabbit renal proximal tubules (Messana, *et al.*, 1988). These cells take up GSH in response to tBHP-induced oxidative stress and hence gain a greater intracellular reducing capacity to neutralise the effects of tBHP. Treatment of A549 human small cell lung carcinoma fibroblasts with the glutathione synthesis inhibitor L-buthionine-(*S,R*)-sulfoximine decreases intracellular GSH and GSSG, but does not perturb the intracellular GSH-to-GSSG ratio, whilst incubation of cells with exogenous GSH has no affect on the intracellular concentrations of either GSH or GSSG (Pendergrass, *et al.*, 1999). On the other hand, incubation of rat heart myocytes with extracellular GSSG, but not GSH, increases intracellular GSH concentrations. Extracellular GSSG raises intracellular GSH concentrations via entry into the cell as GSSG, followed by reduction (Guarnieri, *et al.*, 1987).

The effect of extracellular GSH on intracellular GSH in RBCs has been investigated in a number of studies, although, there appears to be little consistency in the findings. For instance, extracellular GSH has been reported to increase intracellular GSH in

human RBCs through the release of GSH from membrane bound intracellular GSSR (Ciriolo, *et al.*, 1990; Ciriolo, *et al.*, 1993). In contrast, Russell and co-workers (1994) found that extracellular GSH had no effect on intracellular GSH levels, but that the thiol containing antioxidant drugs, *N*-acetylcysteine and captopril, increased intracellular GSH and GSSG, respectively, without changing the total glutathione content.

NMR has frequently been used to observe changes in intra- and extracellular glutathione concentrations (Brown, *et al.*, 1977; Rabenstein, *et al.*, 1985; Reglinski, *et al.*, 1988b; Ciriolo, *et al.*, 1990; Ciriolo, *et al.*, 1993; Rae, *et al.*, 1993; Russell, *et al.*, 1994; Willis and Schleich, 1996; Spickett, *et al.*, 1998). It is ideally suited to monitoring sensitive thiol-containing compounds in whole cells under near *in vivo* conditions. The application of the spin-echo pulse sequence to RBC suspensions results in the simplification of the NMR spectrum to the signals from small, highly mobile molecules (Brown, *et al.*, 1977). As intra- and extracellular GSH and GSSG peaks are coincident in ^{1}H spin-echo spectra at physiological pH, it can be difficult to determine if the reaction is occurring inside or outside the cells. Previous studies have either used chemical shift reagents and cell dilution (Ciriolo, *et al.*, 1990; Ciriolo, *et al.*, 1993), or careful accounting of peak intensities (Russell, *et al.*, 1994) to resolve intra- and extracellular phenomena and determine whether intracellular GSH was affected by exogenous GSH.

3.2 Motivation

The aim of the work reported in this Chapter was to resolve conflicting conclusions as to whether reducing equivalents from GSH can enter the human RBC and reduce GSSG. This was investigated by using spectrophotometric assays, as well as a synthetic ^{13}C isotopomer of GSH, together with the employment of a special feature of heteronuclear NMR spectroscopy, to analyse the effect of extracellular GSH on human RBCs exposed to tBHP. The use of [*glycyl*-2-^{13}C]GSH enabled the direct observation of the oxidation state of extracellular glutathione. In combination with results from ^{1}H spin-echo NMR and spectrophotometric assays, this led to the

conclusion that extracellular GSH does not affect the intracellular GSH-to-GSSG ratio of RBCs exposed to tBHP.

3.3 Results

3.3.1 tBHP oxidation of intracellular GSH

The oxidation of intracellular GSH by tBHP imposes oxidative stress on RBCs (Brown, *et al.*, 1977; Foldes-Papp and Mareyzki, 1984; Rabenstein, *et al.*, 1985; Lapshina and Bartosz, 1995; Zavodnik, *et al.*, 1998; Ingrosso, *et al.*, 2000; Zou, *et al.*, 2001). The oxidation occurs via a GSHPx catalysed reaction (Srivastava, *et al.*, 1974). In order to return GSSG to the reduced state via the NADPH-dependent GR (Figure 3.1), metabolites from glucose oxidation are required (Tietze, 1969; Srivastava, *et al.*, 1974).

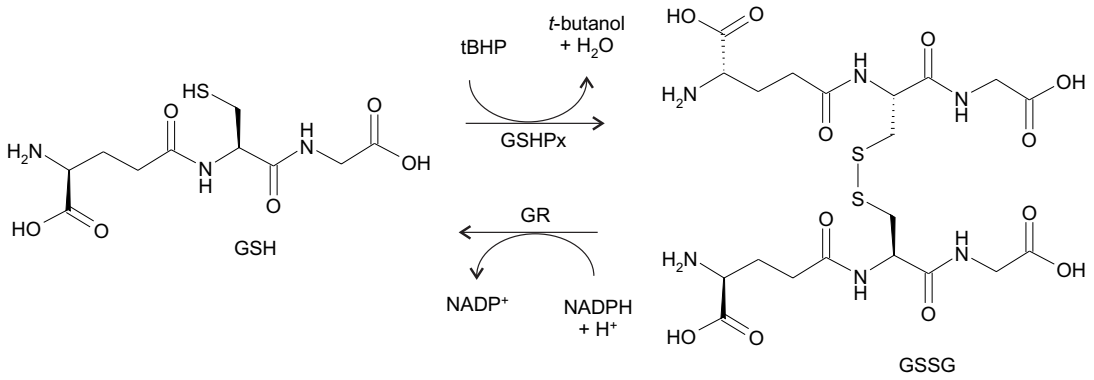

Figure 3.1: Oxidation of GSH in presence of tBHP.

Although the oxidation of GSH by tBHP is enzyme catalysed, tBHP has been shown to have other effects in the cell; it can also lead to increased lipid peroxidation and oxidation of protein thiols (Zavodnik, *et al.*, 1998). Hence, the exact relationship of tBHP concentration to GSH oxidation was investigated. As shown in Figure 3.2, one equivalent of tBHP does not oxidise one equivalent of GSH. When the data were fitted by linear regression it was deduced from the extrapolation that GSH should be fully oxidised at 1.52 ± 0.06 equivalents of tBHP.

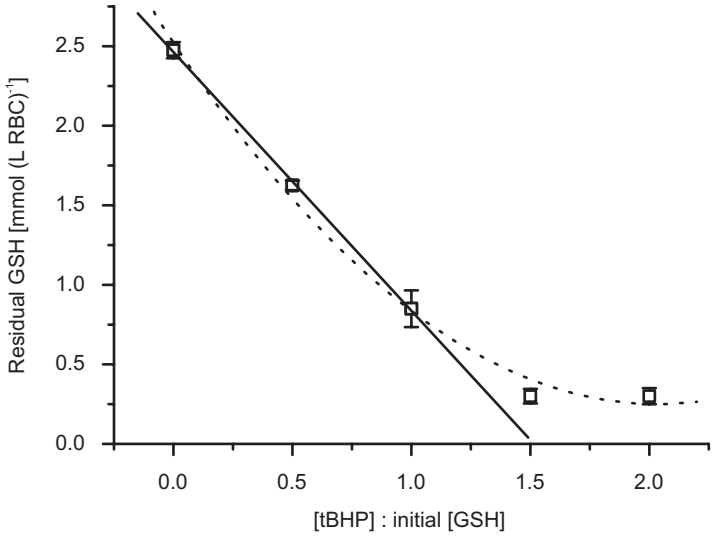

Figure 3.2: Concentration of tBHP required for GSH oxidation. RBC, Hc = 0.7, with initial GSH concentration of 2.5 mmol (L RBC)$^{-1}$, were incubated with increasing concentrations of tBHP; 0–5 mmol (L RBC)$^{-1}$. Data points represent the average of duplicate experiments with error bars denoting ± 1 s.d. Details of the glutathione assay are given in §2.4.1.

3.3.2 Suitability of GSH assay technique

To measure intra- and extracellular GSH concentrations accurately in RBC suspensions supplemented with GSH, the cells had to be quickly and reliably separated from the suspension medium. Conventional centrifugation of RBCs did not provide sufficiently rapid or complete separation, resulting in estimated intracellular GSH concentrations that were significantly higher than those in controls (Figure 3.3). The addition of dibutyl phthalate, which has a density that lies between the densities of the two components of the RBC suspension, to the sample prior to centrifugation, improved the separation. There was no difference in the measured intracellular GSH concentration in control RBC and concentrations in the presence of GSH centrifuged through dibutyl phthalate (Figure 3.3). Measurements of GSH concentrations in the supernatant fractions were less reproducible than those in the cellular fraction. Hence, GSH was only routinely assayed in the cellular fraction.

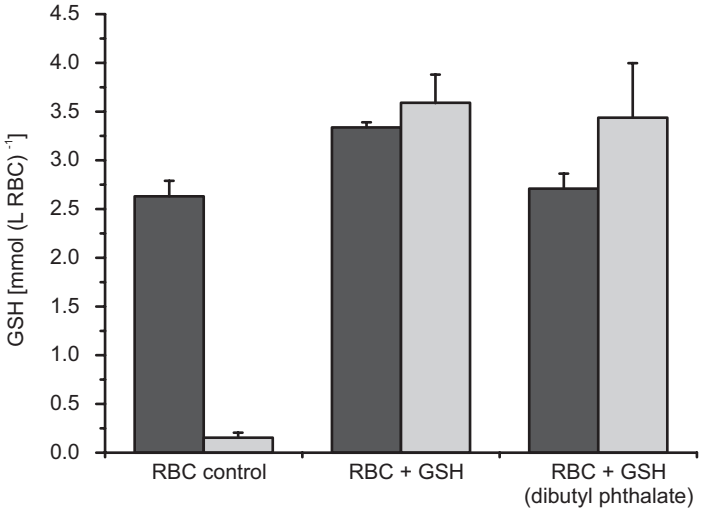

Figure 3.3: Suitability of dibutyl phthalate separation technique for measuring intra- and extracellular GSH concentrations. RBC, Hc = 0.62, were incubated at 25 °C with or without 3.5 mmol (L RBC)$^{-1}$ GSH for 1 min prior to separation by centrifugation for 1 min at 12000 g. "RBC + GSH (dibutyl phthalate)" had 100 µL dibutyl phthalate added prior to centrifugation to ensure separation of RBCs from the supernatant. Packed cells (■) and supernatant (■) were assayed for GSH content. Columns represent the averages of triplicate experiments except that for "RBC + GSH (dibutyl phthalate)" which was the average of six experiments. Error bars denote ± 1 s.d. Details of the glutathione assay are given in §2.4.1.

3.3.3 Effect of extracellular GSH on intracellular GSH concentrations

Incubation of RBCs with the peroxide tBHP decreased the concentration of intracellular GSH (Figure 3.4). In the presence of glucose, GSH oxidised by tBHP returns to control levels within 30 min (Srivastava, *et al.*, 1974). However, in the absence of glucose, as observed here, GSSG was not reduced. The addition of GSH (at a concentration resembling the physiological intracellular concentration) to the cell suspension had no effect on the reduction of GSSG in glucose starved cells exposed to tBHP (intracellular GSH levels did not recover). In the absence of tBHP, RBCs with GSH added to the supernatant displayed the same intracellular GSH concentrations as controls (Figure 3.4).

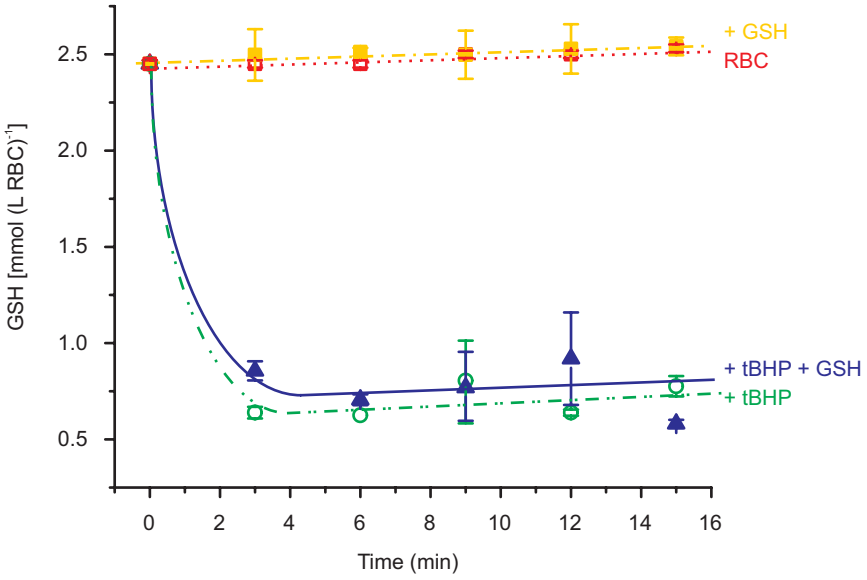

Figure 3.4: Intracellular GSH concentration of glucose-starved human RBCs. RBCs, Hc = 0.7, were incubated in PBS at 25 °C with no additions (□), 2.5 mM GSH (■); 2.5 mM tBHP (○); and 2.5 mM tBHP and 2.5 mM GSH (▲). Glutathione concentrations were measured as reported in §2.4.1. Data points represent the average of two experiments performed in tandem with error bars representing ± 1 s.d.

The addition of 2.5 mmol (L RBC)$^{-1}$ NADH or NADPH to the suspension medium had no effect on the intracellular concentration of GSH in RBC controls or on the recovery of GSH after tBHP exposure, suggesting that the structural integrity of the cell membrane was retained in spite of the addition of tBHP. If NADH or NADPH had been able to enter the glucose-starved cells GR could have reduced GSSG and the intracellular GSH concentration would have increased.

The RBCs used for NMR experiments are generally treated with carbon monoxide to convert oxy/deoxy-Hb to carbon monoxy-Hb which, due to its stable diamagnetic nature, provides maximum resolution in NMR spectra (Himmelreich and Kuchel, 1997). Exposure of RBCs to carbon monoxide prior to the GSH assay had no effect on the results reported above. Hence the NMR results shown below are comparable to those from the spectrophotometric analysis.

3.3.4 Effect of tBHP on NMR spectra of RBCs

In a ^{1}H spin-echo NMR spectrum of a suspension of RBCs, a number of GSH peaks are identifiable (Figure 3.5A) (Brown, *et al.*, 1977). On the addition of tBHP the peaks corresponding to the glutathione protons from Gly αC$\underline{H}_2$, Cys βC$\underline{H}_2$ and γGlu γC$\underline{H}_2$ decreased in absolute intensity. The peak due to γGlu βC$\underline{H}_2$ is relatively unaffected by the oxidation of intracellular GSH (Figure 3.5B). The ratio of the peak intensity of Gly αC$\underline{H}_2$ to γGlu βC$\underline{H}_2$ can be used as an indication of the intracellular GSH-to-GSSG ratio (Kuchel, *et al.*, 1984), with a higher peak ratio corresponding to a greater proportion of total glutathione in the reduced state.

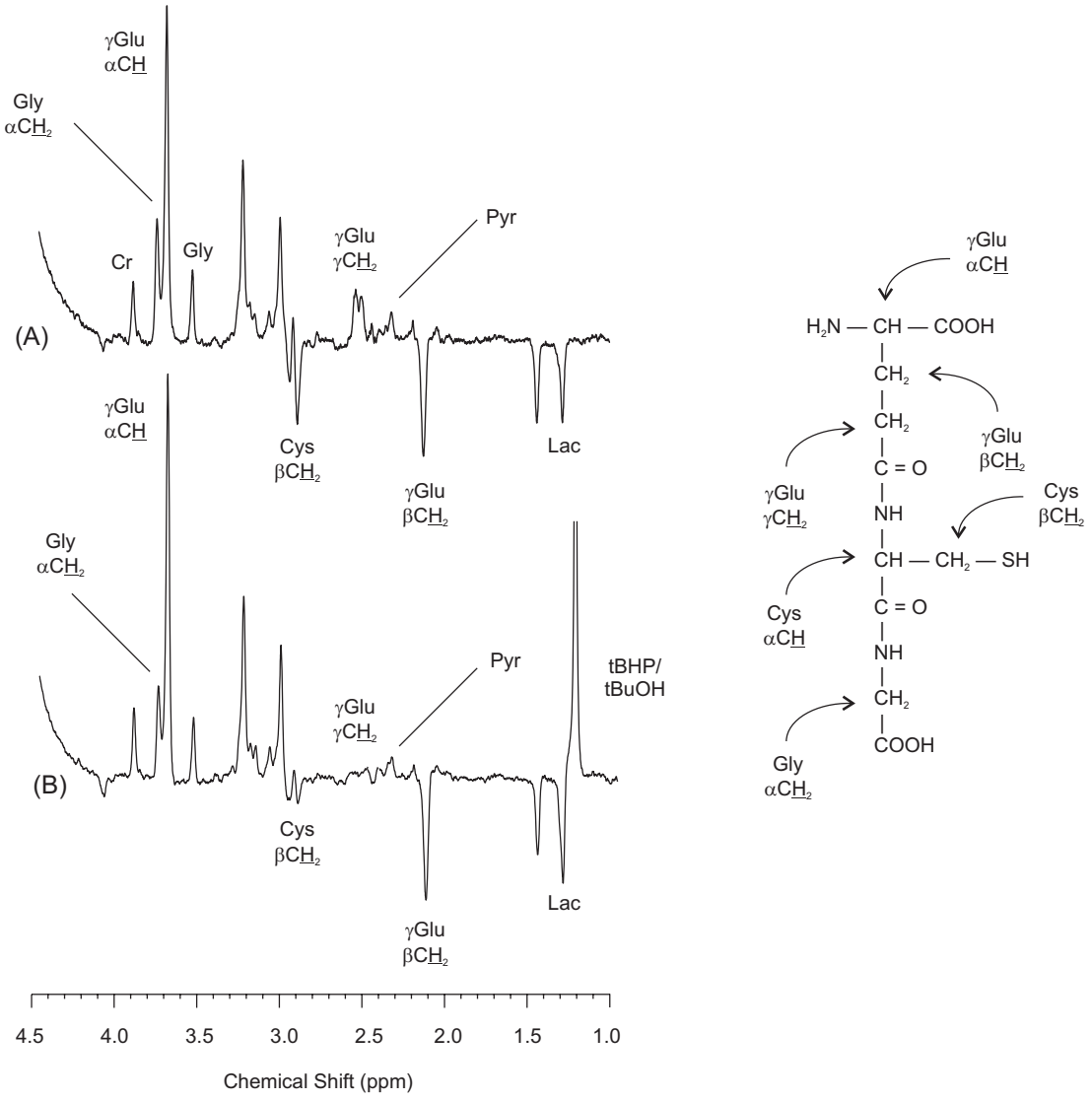

Figure 3.5: Aliphatic region of ^{1}H spin-echo NMR spectra of human RBC suspensions. The structure of glutathione is given for ease of reference to the spectral assignments. **(A)** Glucose-starved RBCs in 2 mM PBS, pH 7.4; **(B)** suspension from **(A)** after incubation for 5 min at 37 °C with 2.5

mmol (L RBC)$^{-1}$ tBHP. Abbreviations used: Cr, creatine; Lac, lactate; Pyr, pyruvate. Data were acquired on a Bruker DRX-600 spectrometer; acquisition details are given in §2.5.3.

One of the difficulties of using ^{1}H spin-echo NMR to investigate changes in intra- and extracellular GSH is the inability to distinguish the species in each location in the cell suspension. To surmount this [*glycyl*-2-^{13}C]GSH was used as the extracellular source of GSH for NMR experiments.

3.3.5 ^{1}H and ^{13}C NMR spectra of [glycyl-2-^{13}C]GSH

[*Glycyl*-2-^{13}C]GSH was synthesised using Fmoc methodology by Dr Paramjit Bansal, University of Queensland. The purified product was subjected to 2D NMR analysis to identify any contaminants and to confirm the location of the ^{13}C label.

^{1}H and ^{13}C chemical shifts for GSH at several pH values have been published (Rabenstein and Keire, 1989). The chemical shifts and the multiplet patterns of the GSH peaks are pH (or pD) dependent due to conformational changes and the electronic influence of the titratable carboxyl, sulfhydryl and ammonium groups (Rabenstein and Keire, 1989). The ^{1}H and ^{13}C chemical shifts for [*glycyl*-2-^{13}C]GSSG at pD 7.56, are expressed relative to [2-^{13}C]formate and represent the midpoints of crosspeaks in HSQC spectra. Since GSH is readily oxidised in solution by molecular oxygen and as 2D NMR experiments often have long acquisition times, [*glycyl*-2-^{13}C]GSH was oxidised to [*glycyl*-2-^{13}C]GSSG by treatment with molecular oxygen to ensure that the spectra were obtained for a single species.

The position of the ^{13}C label was confirmed by double quantum filtered ^{1}H-^{1}H COSY (Figure 3.6), ^{1}H-^{13}C HSQC (Figure 3.7) and ^{1}H-^{13}C HMBC (Figure 3.8) spectra. Although only the Gly α-carbon of [*glycyl*-2-^{13}C]GSSG was labeled with ^{13}C, correlations due to ^{13}C at natural abundance for the other carbon atoms can be observed in these latter two spectra, though at lower signal to noise. The two protons of Gly CH_2 are non-equivalent at pHs other than pH 7.38 and give rise to AB splitting patterns with J_{AB} between -17.74 and -16.92 Hz (Rabenstein and Keire, 1989). The presence of a ^{13}C label at this position introduces an additional splitting.

Two ABX quartets were observed in the ^{1}H NMR spectra of [*glycyl*-2-^{13}C]GSSG. The calculated chemical shifts and *J*-couplings of the protons are shown in Table 3.1 and are in agreement with literature values for GSSG. The intense peaks in the ^{1}H-^{13}C HSQC (Figure 3.7) and ^{1}H-^{13}C HMBC (Figure 3.8) spectra at the corresponding chemical shifts confirmed the labelling pattern of GSH. An additional doublet, with J = 138.96 Hz and centred at $\delta(^{1}H)$ 3.76, may be from free Fmoc[2-^{13}C]Gly. However the intensity of the peak was too low for complete characterisation. An ABX splitting pattern is also observed for the methylene protons of the cysteine residue. These protons are diastereotopic and have different chemical shifts at pH 7.37 for both GSH (υ_A = 2.959; υ_B = 2.922; $\Delta\upsilon$ = 0.037 ppm) and GSSG (υ_A = 3.296; υ_B = 2.965; $\Delta\upsilon$ = 0.331 ppm) (Rabenstein and Keire, 1989). The chemical shifts and *J*-couplings calculated from the ^{1}H NMR spectrum are shown in Table 3.1. The chemical shifts and $\Delta\upsilon$ = 0.331 for the labelled glutathione are in agreement with the literature values for GSSG, confirming that the [*glycyl*-2-^{13}C]glutathione was completely oxidised prior to acquisition of the chemical shift data (Table 3.2).

Table 3.1: Chemical shifts and coupling constants for the ABX spin systems of [*glycyl*-2-^{13}C] GSSG at pH 7.56 calculated from ^{1}H NMR spectra and from Rabenstein and Keire (1989) for GSSG at pH 7.37.

	[*glycyl*-2-^{13}C]GSSG, pH 7.56		GSSG, pH 7.37	
	Gly $\alpha^{13}CH_2$	Cys βCH_2	Gly αCH_2	Cys βCH_2
υ_A (ppm)	3.780	3.292	3.778	3.296
υ_B (ppm)	3.746	2.959	3.745	2.965
$\Delta\upsilon$	0.034	0.332	0.033	0.331
J_{AB} (Hz)	-17.3	-14.3	-17.37	-14.29
J_{AX} (Hz)	139.55	4.53		4.13
J_{BX} (Hz)	139.20	9.59		9.65

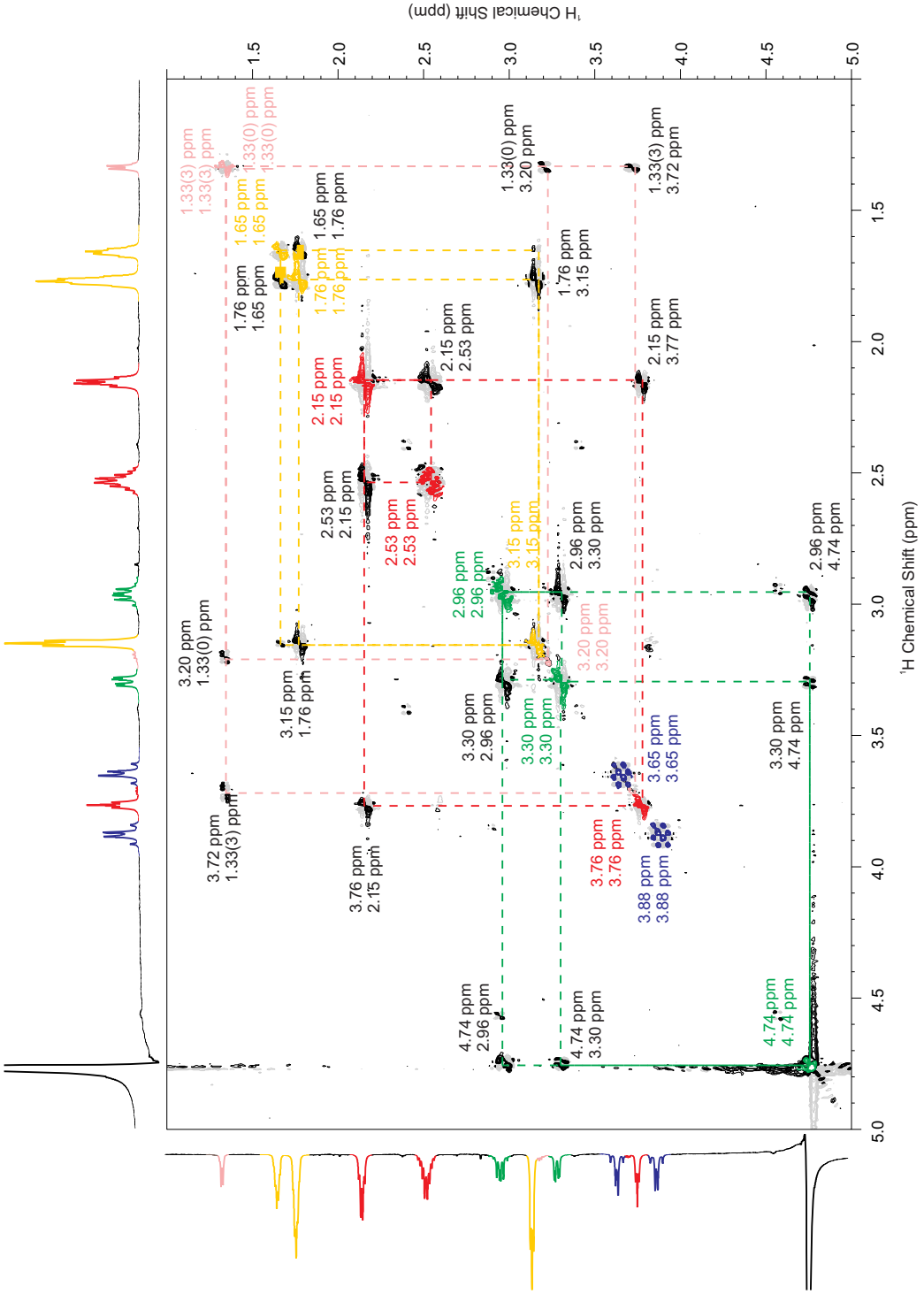

Figure 3.6: ^{1}H double quantum filtered COSY spectrum of [*glycyl*-2-^{13}C] GSSG. [*Glycyl*-2-^{13}C]GSH was dissolved in D_2O to a concentration of 1.55 mM, adjusted to pH 7.5 and 290 mOsmol kg^{-1} and converted to the oxidised form by exposure to O_2. The peaks corresponding to the glutathione amino acid residues are colour coded: γGlu (red), Cys (green) and Gly (blue). Peaks from the main contaminant (piperidine) are coloured yellow and those of the minor contaminant are in pink. ^{1}H-^{1}H couplings are indicted by the dashed lines. Details of spectral acquisition parameters are described in §2.5.2.

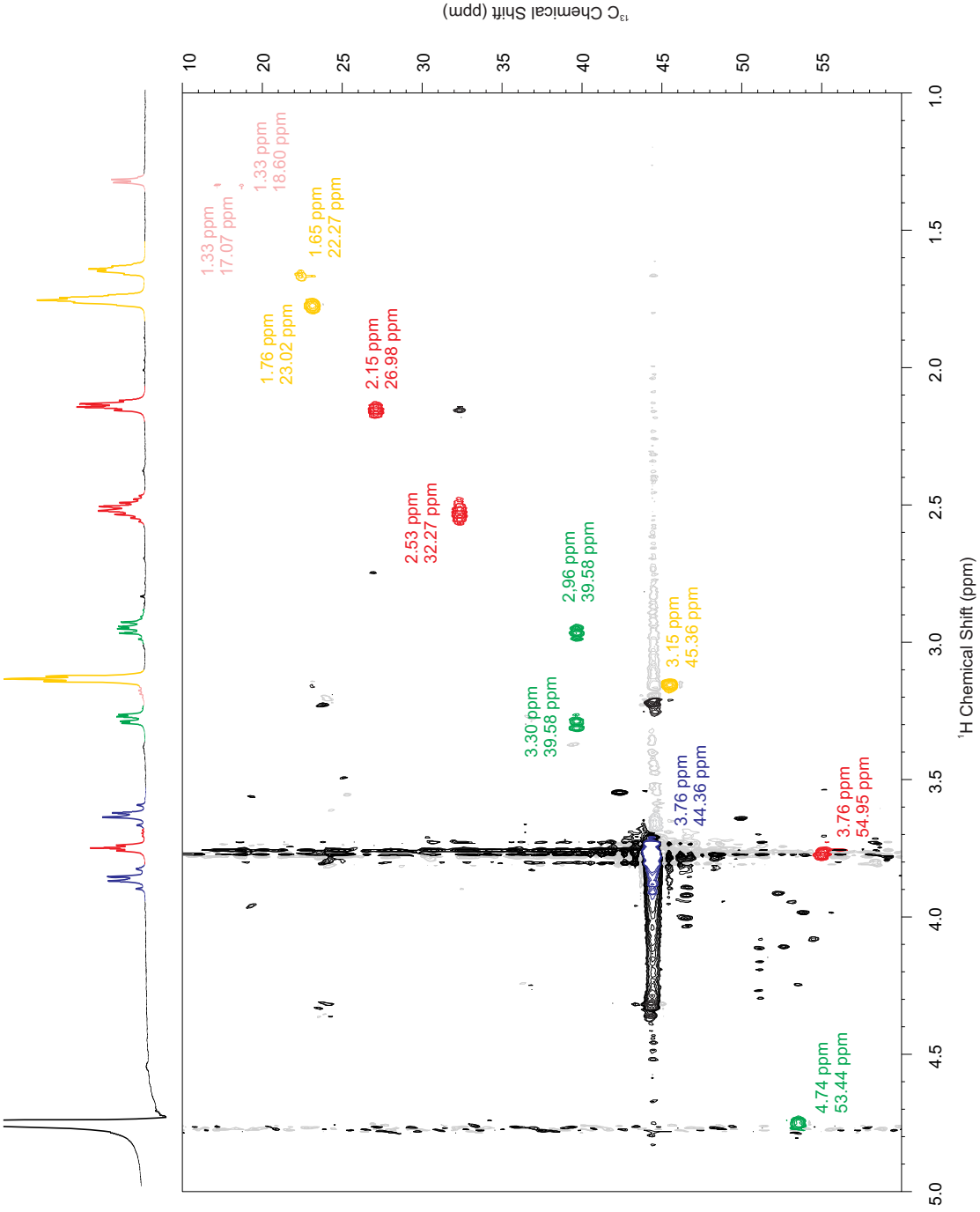

Figure 3.7: ^{1}H-^{13}C HSQC spectrum of [*glycyl*-2-^{13}C] GSSG. [*Glycyl*-2-^{13}C]GSH was dissolved in D_2O to a concentration of 1.55 mM, adjusted to pH 7.5 and 290 mOsmol kg^{-1} and converted to the oxidised form by exposure to O_2. The peaks corresponding to the glutathione amino acid residues are colour coded: γGlu (red), Cys (green) and Gly (blue). Peaks from the main contaminant (piperidine) are coloured yellow and those of the minor contaminant are in pink. Details of spectral acquisition parameters are described in §2.5.2.

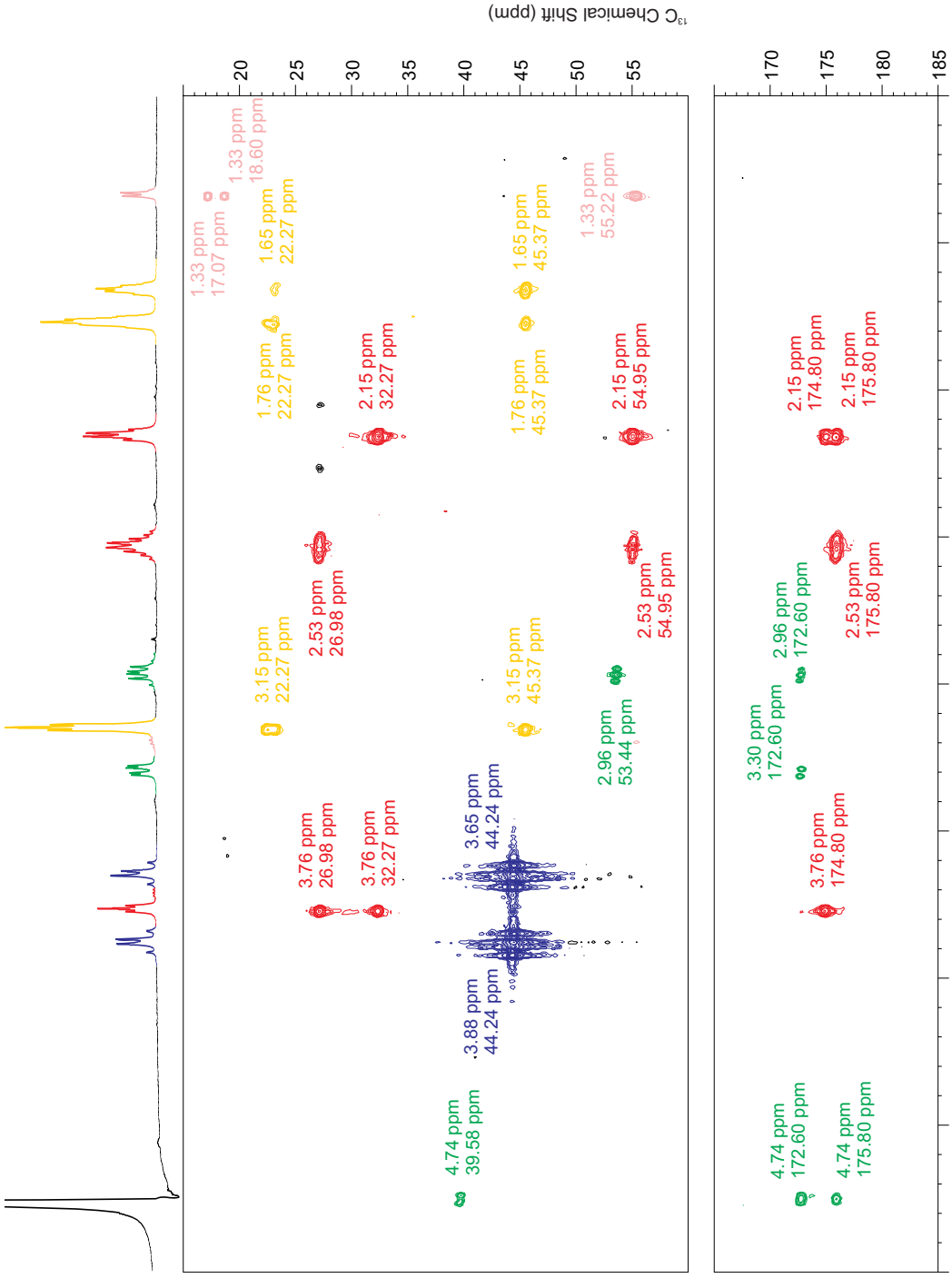

Figure 3.8: ^{1}H-^{13}C HMBC spectrum of [*glycyl*-2-^{13}C]GSSG. [*Glycyl*-2-^{13}C]GSH was dissolved in D_2O to a concentration of 1.55 mM, adjusted to pH 7.5 and 290 mOsmol kg^{-1} and converted to the oxidised form by exposure to O_2. Peaks corresponding to the glutathione amino acid residues are colour coded: γGlu (red), Cys (green) and Gly (blue). Peaks from the main contaminant (piperidine) are coloured yellow and those of the minor contaminant are in pink. Details of spectral acquisition parameters are described in §2.5.2.

Table 3.2: ^{1}H and ^{13}C chemical shift assignments for [*glycyl*-2-^{13}C]GSSG at pH 7.5

	Measured chemical shift (ppm)		Literature chemical shift (ppm)[a]		Chemical structure
	^{1}H	^{13}C	^{1}H	^{13}C	
γGlu αCOOH	-	174.8	-	174.6	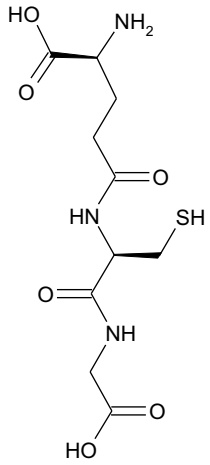
γGlu αCH	3.76	54.95	3.769	55.20	
γGlu βCH_2	2.15	26.98	2.152	27.2	
γGlu γCH_2 (H_A)	2.53[b]	} 32.27	2.545	} 32.4	
γGlu γCH_2 (H_B)	2.53[b]		2.509		
γGlu γCONH	-	175.8	-	175.6	
Cys αCH	4.74	53.44	4.74	53.58	
Cys βCH_2 (H_A)	3.30	} 39.58	3.296	} 39.79	
Cys βCH_2 (H_B)	2.96		2.965		
Cys αCONH	-	172.60	-	172.40	
Gly $\alpha^{13}CH_2$ (H_A)	3.88	} 44.36	3.778	} 44.50	
Gly $\alpha^{13}CH_2$ (H_B)	3.65		3.747		
Gly αCOOH*	-	not observed	-	176.9	

[a] GSSG chemical shifts are from Rabenstein and Keire (1989). For ^{1}H NMR spectra GSSG was dissolved in D_2O at pH 7.37; for ^{13}C NMR spectra GSSG was in D_2O at pH 6.98.

[b] The chemical shifts for γGlu γCH_2-H_A and H_B were taken as the centre of the multiplet as the ABM_2X splitting pattern can not be analysed directly from the spectrum.

3.3.6 Identification of contaminants in [glycyl-2-^{13}C]GSH

The ^{1}H COSY spectrum (Figure 3.6) showed that the [*glycyl*-2-^{13}C]GSH preparation contained a number of contaminants. The major contaminant, coloured yellow, contained three groups of *J*-coupled protons. Integration of the ^{1}H NMR spectrum indicated that the peaks at 3.15, 1.76, and 1.65 ppm were in the ratio 2:2:1. The corresponding carbon chemical shifts were determined from the ^{1}H-^{13}C HSQC spectrum (Figure 3.7) as δ(^{13}C) 45.37, δ(^{13}C) 23.02 and δ(^{13}C) 22.27, respectively. These chemical shifts are consistent with the contaminant being piperidine (Table 3.3; Morishima, *et al.*, 1971; Morishima, *et al.*, 1975), which was used to remove

protecting groups in the synthesis of [*glycyl*-2-^{13}C]GSH. Piperidine was found to have no effect on cell morphology or the extent of lysis at concentrations between 0.001 mM and 10 mM (data not shown), and so was not removed prior to addition of the labelled GSH to RBC suspensions.

The minor contaminant, coloured pink in the spectra, was too low in concentration to enable full assignment. However, based on the observed ^{1}H and ^{13}C chemical shifts and some observed connectivities it is possible that these signals were due to *N,N*-diisopropylethylamine (Table 3.3), which was used to activate the amino acids during the Fmoc synthesis of [*glycyl*-2-^{13}C]GSH.

Table 3.3: ^{1}H and ^{13}C chemical shift assignments for the two main contaminants piperidine and *N,N*-diisopropylethylamine.

	Measured chemical shift (ppm)		Literature chemical shift (ppm)		Chemical structure
	^{1}H	^{13}C	^{1}H	^{13}C	
Piperidine					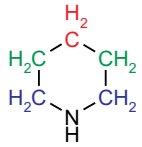
CH_2-4 (red)	1.65	22.27	1.54[a]	25.2[b]	
CH_2-3,5 (green)	1.76	23.02	1.54[a]	27.8[b]	
CH_2-2,6 (blue)	3.15	45.37	2.80[a]	46.9[b]	
***N,N*-diisopropylethylamine**					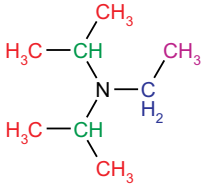
Isopropyl CH_3 (red)	1.333	17.07 18.60	1.011[c]	19.36[d]	
Isopropyl CH (green)	3.72	55.22	3.017[c]	52.41[d]	
Ethyl CH_2 (blue)	3.20		2.467[c]	41.98[d]	
Ethyl CH_3 (purple)	1.330		1.02[c]	15.23[d]	

[a] Piperidine in 10% $CDCl_3$ referenced to internal standard of Me_4Si (Morishima, *et al.*, 1975)

[b] Piperidine in 50% $CDCl_3$ referenced to internal standard of CS_2 (Morishima, *et al.*, 1971)

[c] *N,N*-diisopropylethylamine in $CDCl_3$ referenced to external TMS (SDBSWeb: http://www.aist.go.jp/RIODB/SDBS/)

[d] *N,N*-diisopropylethylamine in D_2O referenced to external TMS (Sarneski, *et al.*, 1975)

3.3.7 Measurement of intra- and extracellular GSH by NMR

^{13}C labelling of GSH in the glycyl C-2 position gives rise to a splitting of the proton resonances from Gly α$^{13}CH_2$ due to $^1J_{C,H}$ coupling with the NMR-active ^{13}C nucleus (Figure 3.9A). In ^{1}H spectra from unlabelled GSH this resonance appears as a singlet (Figure 3.9B). Hence, labelled and unlabelled GSH are in principle distinguishable in this chemical shift region.

However, on addition of [*glycyl*-2-^{13}C]GSH to an RBC suspension, the Gly α$^{13}CH_2$ splitting was not discernible due to overlap with resonances from creatine and glycine. Thus, although changes in the intracellular (unlabelled) GSH redox state can be monitored through changes in the relative intensity of the Gly αCH_2 resonance in ^{1}H spin-echo NMR spectra, the oxidation state of the extracellular GSH could not be determined from these experiments alone. Instead, on the reasonable assumption that natural abundance effects could be safely ignored for the short experiment times that were used, changes in the redox state of the extracellular (labelled) GSH were followed by using ^{13}C[^{1}H-decoupled] NMR, where spectra of [*glycyl*-2-^{13}C]GSH and GSSG were seen to be distinguishable (Figure 3.9C, D). Thus, changes in the oxidation state of both the endogenous (unlabelled), and exogenous (labelled), glutathione were measured sequentially and non-disruptively.

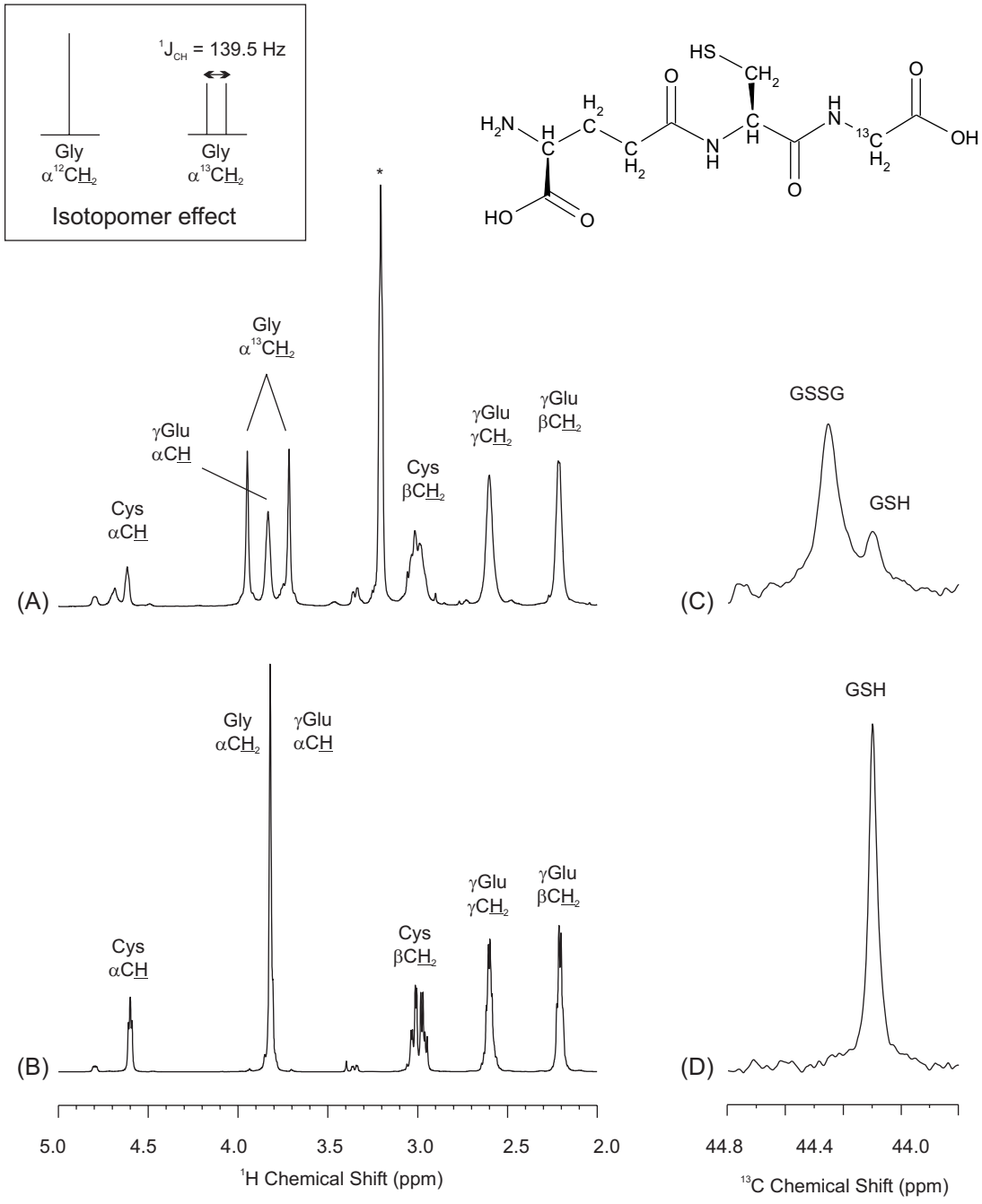

Figure 3.9: ^{1}H and ^{13}C NMR spectra of [*glycyl*-2-^{13}C] and unlabelled glutathione. The insert shows the isotopomer effect for the Gly ^{13}C$\underline{H}_2$. **(A)** ^{1}H NMR spectrum of 50 mM [*glycyl*-2-^{13}C]GSH (see structure), pH 7.7; **(B)** ^{1}H NMR spectrum of 50 mM GSH (unlabelled) pH 7.7; **(C)** ^{13}C[^{1}H-decoupled] NMR spectrum of a mixture of 0.66 mM [*glycyl*-2-^{13}C]GSH and 1.55 mM [*glycyl*-2-^{13}C] GSSG, pH 7.4; **(D)** ^{13}C[^{1}H-decoupled] NMR spectrum of 7.56 mM [*glycyl*-2-^{13}C]GSH, pH 7.4. Spectra were acquired on a Bruker DRX-600 spectrometer, acquisition details are given in §2.5.3. The * denotes the C$\underline{H}_2$, H-6 resonance from the major contaminant piperidine in the [*glycyl*-2-^{13}C]GSH preparation (additional resonances at 1.76 and 1.65 ppm not shown).

3.3.8 Effect of extracellular GSH on intracellular GSH and metabolism in intact RBC

^{1}H spin-echo NMR experiments on tBHP-exposed glucose-starved RBCs indicated that over a 2 h period glutathione became gradually more reduced. The inclusion of [*glycyl*-2-^{13}C]GSH in the extracellular medium increased the initial GSH-to-GSSG ratio above controls, but had no effect on the rate of GSSG reduction (Figure 3.10). Over the same period there was no change in the extracellular GSH-to-GSSG ratio, as measured by ^{13}C[^{1}H-decoupled] NMR.

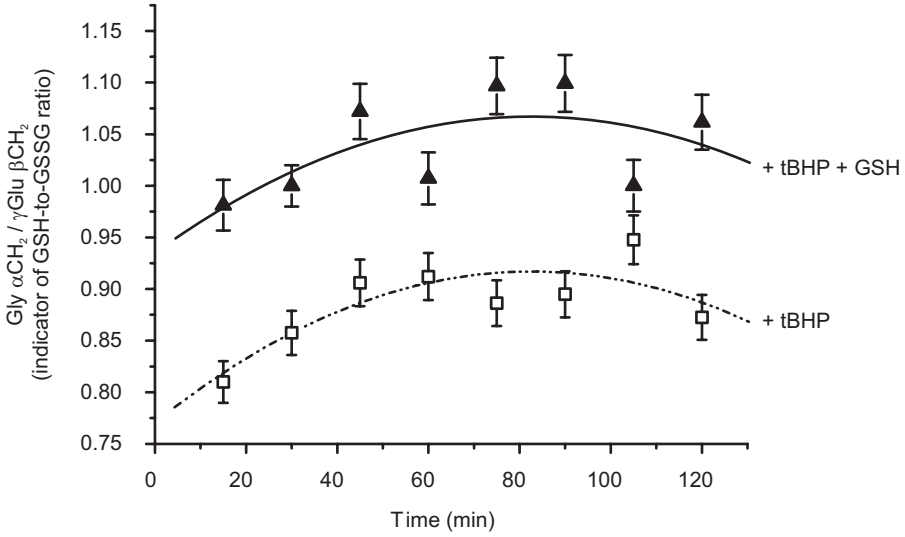

Figure 3.10: Effect of extracellular GSH on ratio of intracellular reduced-to-oxidised glutathione. RBCs, Hc = 0.65, were incubated in PBS at 37 °C with 2.5 mM tBHP (□); and 2.5 mM tBHP and 2.5 mM [*glycyl*-2-^{13}C]GSH (▲). ^{1}H spin-echo NMR spectra were acquired over a 2 h period on a Bruker DRX-600 spectrometer (acquisition information in §2.5.3). The change in the GSH-to-GSSG ratio was determined by dividing the peak integral of the Gly αCH_2 peak by the γGlu βCH_2 peak integral. Empirical quadratic equations were fitted to the data. Error bars represent the coefficient of variance determined from multiple measurements on the same peak.

Extracellular GSH also had little effect on another metabolic marker (the lactate-to-pyruvate ratio) in glucose-starved RBCs exposed to tBHP. The rate of change of the lactate-to-pyruvate ratio, measured by ^{1}H spin-echo NMR, was the same for controls and cells with [*glycyl*-2-^{13}C]GSH in the extracellular medium (Figure 3.11), although the initial lactate-to-pyruvate ratio was lower than that observed for controls.

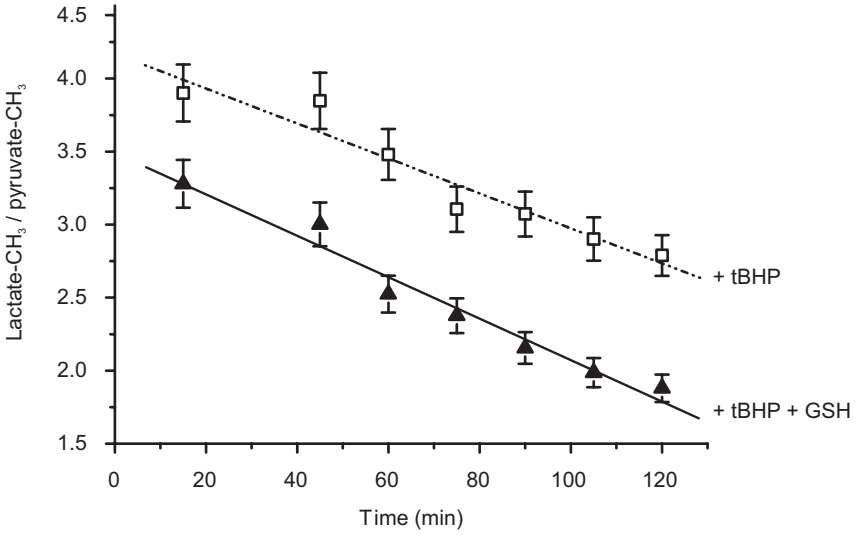

Figure 3.11: Effect of extracellular GSH on the lactate-to-pyruvate ratio. RBCs, Hc = 0.65, were incubated in PBS at 37 °C with 2.5 mM tBHP (□); and 2.5 mM tBHP and 2.5 mM [*glycyl*-2-^{13}C]GSH (▲). ^{1}H spin-echo NMR spectra were acquired over a 2 h period on a Bruker DRX-600 spectrometer (acquisition information in §2.5.3). The change in the lactate-to-pyruvate ratio (B) was determined by dividing the lactate-CH_3 peak integral by the pyruvate-CH_3 peak integral. Data were analysed with the line of best fit. Error bars represent the coefficient of variance determined from multiple measurements on the same peak.

3.4 Discussion

The combination of ^{1}H spin-echo and ^{13}C[^{1}H-decoupled] NMR used in these experiments has provided a simple means of unequivocally distinguishing intra- from extracellular glutathione, and the determination of the glutathione redox state in a non-invasive manner.

Exposure of RBCs to tBHP results in the rapid oxidation of intracellular GSH (Figures 3.4 and 3.5), by a GSHPx catalysed reaction (Srivastava, *et al.*, 1974). To return GSSG to the reduced state via NADPH-dependent GR requires glucose oxidation (Tietze, 1969; Srivastava, *et al.*, 1974). The results obtained here indicate that the presence of extracellular GSH did not lead to an increase in the intracellular GSH concentration in glucose starved cells with or without exposure to tBHP (Figure 3.4). This was in agreement with the corresponding spectrophotometric results of Ciriolo and co-workers (1993) who reported that if GSH-exposed cells were washed before assay no increase in intracellular GSH was observed. However, Ciriolo and

colleagues (1993) also present the contrasting results that if total (intra- and extracellular) GSH was measured, spectrophotometrically or by ^{1}H spin-echo NMR, an increase in total sample GSH over and above the sum of the original cellular GSH and the added extracellular GSH was observed. A possible explanation for their ^{1}H NMR results might have been the alteration of the shape of their cells (brought about by, amongst other things, a change in the osmotic conditions) that in a spin-echo experiment can give rise to variations in total signal intensity even though changes in concentration do not occur (Rae, *et al.*, 1993).

The ^{1}H spin-echo and $^{13}C[^{1}H$-decoupled] NMR data presented here clearly show that incubation of glucose-starved RBCs (exposed to tBHP) with extracellular GSH did not affect the rate of intracellular GSSG reduction (Figure 3.10) or the rate of cellular metabolism (Figure 3.11), confirming the results obtained by spectrophotometric assay. There have been conflicting reports as to whether extracellular GSH can increase the intracellular GSH concentration. Russell and co-workers (1994) found that incubation of RBCs with 0.5 mM GSH for 1 h had no effect on the cytosolic glutathione balance, while Ciriolo and colleagues (1993) reported that 0.5 mM GSH produced a twofold increase in intracellular GSH within 10 min. This increase in intracellular GSH, although transient and removable by washing the cells, was concomitant with an increase in extracellular GSSG. The increase in GSH was explained by the postulated release of GSH from intracellular membrane bound GSSR, through a membrane mediated thiol-disulfide exchange mechanism. GSH in the RBC has previously been reported to be sensitive to the cell impermeable oxidant Ellman's reagent (DTNB), forming GSSR with membrane components with the concomitant reduction of Ellman's reagent (Reglinski, *et al.*, 1988a). This concept was applied in reverse by Ciriolo and colleagues (1993).

Incubation of RBCs with extracellular GSH, although not affecting the change in the GSH-to-GSSG ratio over 2 h, did appear to increase the initial GSH ratio above that observed in controls (Figure 3.10). The added [*glycyl*-2-^{13}C]GSH did not contribute to the observed Gly αCH_2 resonance, but increased the γGlu βCH_2 resonance. Hence, it was expected that the Gly αCH_2 to γGlu βCH_2 ratio observed would be lower than that observed for the control. It is unlikely that this response was caused

by the release of intracellular GSSR, as reported by Ciriolo and colleagues (1993), as the extracellular GSH-to-GSSG ratio measured by $^{13}C[^{1}H$-decoupled] NMR did not change. It may reflect the different initial glutathione concentrations in the control and GSH-exposed cells as the same amount of tBHP was added to both samples.

In conclusion, the results presented here indicate that extracellular GSH has no effect on intracellular GSSG concentrations, the change in intracellular GSH-to-GSSG with time, or the end product of starvation metabolism in glucose-starved RBCs exposed to tBHP.